Observation of Correlated Emission Intensity and Polarization Fluctuations in Single CdSe/ZnS Quantum Dots[†]

Daniel Montiel[‡] and Haw Yang*[,‡,§]

Department of Chemistry, University of California at Berkeley, Berkeley, California, and Physical Biosciences Division, Lawrence Berkeley National Laboratory, Berkeley, California 94720

Received: March 17, 2008; Revised Manuscript Received: June 20, 2008

Time-resolved single-nanoparticle spectroscopy has been carried out to examine the luminescence characteristics of individual CdSe/ZnS core/shell quantum dots. In particular, the possible correlations between emission intensity, lifetime, spectrum, and polarization fluctuations have been investigated. The emission polarization was found to be correlated with the luminescence intensity in a nonlinear way. The low-emissive states were found to correlate with red-shifted spectrum, increased nonradiative decay, and low degree of emission polarization. The observations are consistent with the model that charged quantum dots can be emissive.

1. Introduction

Colloidal semiconductor nanoparticles, or quantum dots, have generated great interest because of their potential use as optical probes for sensing applications and also because of their unusual photophysical behavior. At the single-particle level, the emission intensity of quantum dots switches between periods of high ("on" state) and low ("off" state) intensity, termed blinking.[1] The on/off time statistics of the blinking have been phenomenologically modeled by power-law distribution.[2,3] This blinking of quantum dots has been shown to be correlated with fluctuations in the emission spectrum[4−6] and lifetime.[7,8] More recently, it has been shown that, rather than discrete on/off two states, there is a continuous distribution in the emission intensities and that the intensity is correlated with lifetime in a nonlinear way.[9] In fact, this blinking phenomenon appears to be a general feature of emissive probes at the single-particle or single-molecule level and its underlying physical basis is an active area of research.[10]

The current working hypothesis is that the luminescence quenching (blink off) is due to charging in the quantum dot.[1,11] Models ranging from trapped surface charges to various charge migration modes[2,12−15] have been proposed to explain the dynamics of this time-dependent emission behavior of the quantum dots. In certain models, for example, the nanoparticle is considered to be in the "on" state when the charge is allowed to migrate on the surface, but the particle may "blink off" when the charge(s) travels by a random walk process into the core. Other models based on the idea of diffusion-coupled electron-transfer mechanism predict differences in the photophysical behavior between the microsecond and millisecond time regimes.[16] In addition to the excitation energy,[17] the nanoparticle's local dielectric environment has been shown to affect blinking of quantum dots.[18] For example, the luminescence wavelength can be modified by the Stark effect.[4] Taken together, these observations are consistent with a charged particle model.[19] Along the same vein, localized charges are expected to mitigate a nanoparticle's local dielectric environment such that the polarization of the emitted light, spectrum, and intensity should be correlated in some way. Although previous studies have reported that the time-averaged emission polarization for an immobilized particle does not change,[20,21] it remains unknown if polarization fluctuates dynamically and correlates with luminescence intensity intermittency. It therefore will be of great interest to understand how, if at all, the intensity, luminescence lifetime, polarization, and spectral fluctuations are correlated in a time-dependent manner. The results will aid in gaining a more complete understanding of the fluctuations of optical observables that a single quantum dot can afford. In the present study, individual streptavidin-coated CdSe/ZnS quantum dots were examined with a confocal microscope with the capability to simultaneously measure the lifetime, intensity, color dichroism, and linear dichroism of the emission.

2. Experimental Procedures

An amount of 20 μL of 0.1 nM solution of streptavidin-coated CdSe/ZnS core/shell quantum dots (Invitrogen lot no. 45024A) in isopropyl alcohol was spin-coated onto a quartz coverslip. A 0.1% (weight) poly(methyl methacrylate) (PMMA)/toluene solution was then spin-coated on top of the same coverslip. The coverslip was then placed on a modified Olympus IX70 confocal microscope similar to previous works.[9] The sample was illuminated using 405 nm light from a frequency-doubled Ti: Sapphire laser (Tsunami, Spectra-Physics). A Pockel's cell (M305, Conoptics) was set to pick every 32nd pulse reducing the repetition rate from 80 to 2.5 MHz prior to passing through a type-I BBO doubling crystal (Casix). The light was circularly polarized using a quarter waveplate (Tower Optical). Two band-pass filters (417/60, Semrock), a 25 μm pinhole spatial filter, and a series of neutral density filters were placed in the light path to block the 810 nm fundamental light and attenuate the beam. The average laser power prior to entering the microscope objective was ∼40 nW. Assuming a diffraction-limited focal spot at 405 nm and an ∼50% power reduction by the objective, the density is estimated to be ∼26 W/cm². In the current study, the excitation power density was purposely kept low in order to avoid multiphoton excitation processes and minimize known factors affecting the on-time statistics with high excitation power.[2,12] The collimated light was then reflected off of a long-pass filter (488 DCXR, Chroma) before passing through a 1.3 NA infinity-corrected oil immersion objective (Olympus). The

Luminescence of Single CdSe/ZnS Quantum Dots

J. Phys. Chem. A, Vol. 112, No. 39, 2008 **9353**
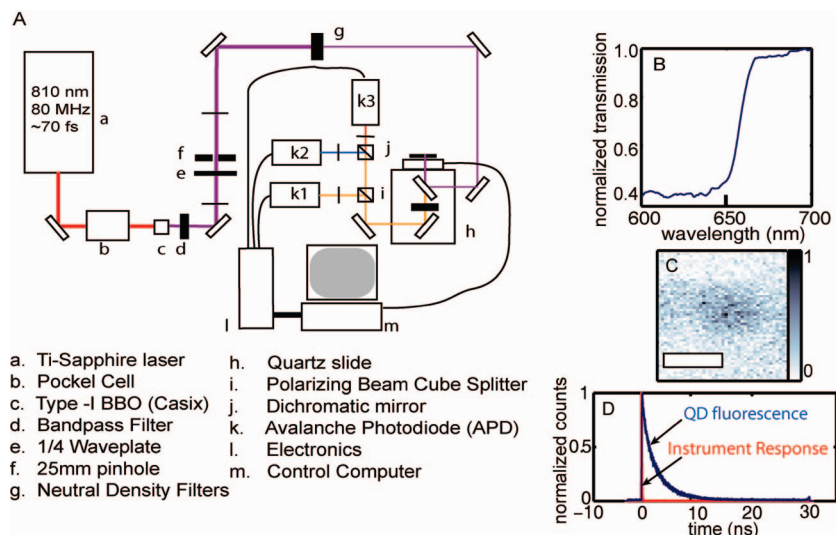

Figure 1. (A) Diagram of the experimental setup. The detector channel numbers are illustrated in the diagram. (B) Normalized transmission spectrum of dichroic in the microscope. The band-edge is located at 658 nm. The spectrum of the dichroic was normalized against the spectrum of the tungsten lamp measured in the absence of the dichroic. The maximum value of the transmission was then normalized to 1. (C) False color image of the diffraction-limited spot of the scanned particle. Scale bar is 300 nm. (D) Lifetime plot showing luminescence decay of the quantum dot (QD) at room temperature (blue) overlaid with instrument response function measured at 405 nm (red), full width half-maximum ∼680 ps.

emitted light was collected by the same objective before passing through a 570 nm long-pass emission filter (E570LP, Chroma). A polarizing beam cube splitter (Newport) with an extinction ratio of 500:1 was used to separate the light into two orthogonal polarizations. The polarization beam splitter seen in Figure 1A serves two purposes: (i) it separates the light into two separate polarizations, and (ii) it serves as a linear polarizer to account for the polarization dependence of the dichromatic mirror. Note that the complications in quantifying polarization measurements through a microscope objective[22−24] do not play a significant role here because the present work focuses on the correlation between emission intensity and linear dichroism. The transmitted light through the polarization beam splitter was spectrally resolved by a dichromatic mirror (650DCRX, Chroma) with a band-edge empirically set at 658 nm (Figure 1B). The transmission spectrum of the dichroic was measured on the transmitted axis with a calibrated spectrometer. The light on each of the three axes were focused by a 75 mm lens onto three single photon counting avalanche photodiode modules (SPCM-AQRH-14, Perkin-Elmer) with measured response times of 680 ps at 405 nm (Figure 1A). The information from each of the detectors was sent through a discriminator, level translator, and delay lines (electronic components in Figure 1A, part l) before finally being collected by a time-correlated single photon counting card (SPM-600, Becker & Hickel), which recorded the absolute photon arrival time, the excitation−emission delay time (microtime), and detector channel number. A piezoelectric stage with a range of 40 μm × 40 μm was used to raster scan the sample over the illumination volume. Raster scanned images of the quantum dots prior to data collection yielded a diffraction-limited spot on all three channels (Figure 1C).

Once possible dots were identified, the diffraction-limited spots were centered over the illumination volume for time-dependent data collection for at least 5 min. A typical intensity−time trajectory is shown in Figure 2B. From the selected trajectories, the photon arrival times of all three channels were then analyzed using a change-point analysis algorithm[9,25,26] to detect and locate discrete intensity change points. Change-point segments, defined as the time trace between two successive intensity change points, were isolated for further
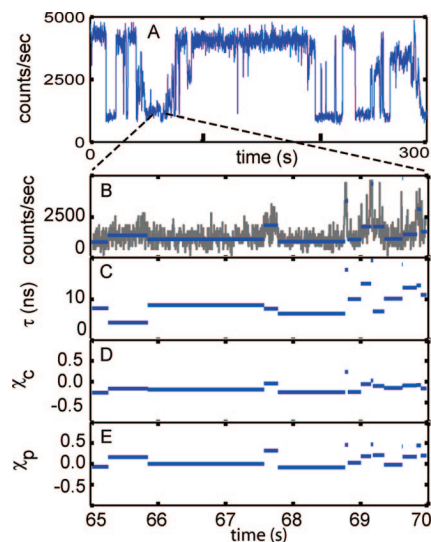

Figure 2. (A) Typical quantum dot (QD) trajectory qualitatively displaying two dominant states. (B−D) Respectively, values of the intensity, luminescence lifetime, color dichroism, and linear dichroism are calculated over time segments identified by change-point analysis and plotted as a function of time.

analysis. The lifetime, color dichroism, polarization dichroism, and intensity were calculated over each segment. For each quantum dot, joint probability distribution maps weighted by the segment duration were calculated to examine the correlation among these four parameters.

3. Discussion

The fluctuations of the luminescence intensity, lifetime, spectrum, and polarization were studied using a time-resolved confocal microscope as has been discussed in a previous work.[9] The simultaneous examination of the polarization and spectrum observables was accomplished using three avalanche photodiodes (Figure 1A). In this configuration, the total intensity was calculated by considering the photons from all three detectors:

$$I_{total} = I_1 + I_2 + I_3$$

The linear dichroism and color dichroism were used to examine the polarization and spectral fluctuations, respectively. These were defined as

$$\chi_p = \frac{I_1 - (I_2 + I_3)}{I_{total}}$$

$$\chi_c = \frac{I_2 - I_3}{I_2 + I_3}$$

Therefore, $\chi_c < 0$ for red-shifted emission and $\chi_c > 0$ for blue-shifted emission. Once the microscope was centered over a particle of interest, the absolute photon arrival times, microtimes, and channel numbers were recorded. The durations between successively detected photons from all detectors were then processed using a likelihood ratio-based change-point segmentation algorithm.[25] The output of this algorithm is a series of photon indices corresponding to the most likely locations of where a change in the Poisson distribution of the photon arrival times has occurred. In the segments between two consecutive change points, the values of the linear and color dichroism were calculated. This approach has been used before to examine the correlation between the intensity and lifetime.[9] In the current configuration, the linear dichroism and color dichroism were correlated with the lifetime and total intensity.

In order to examine possible correlations between the different parameters, joint probability maps are constructed for each pair of parameters. The distribution plot represents a two-dimensional probability map between the lifetime and intensity calculated from the single-particle emission trajectories. The probability density correlating two parameters p_1 and p_2 is calculated by

$$P(p_1, p_2) = \frac{1}{t_{total}} \sum_{j=1}^{N} t_j \frac{1}{\sigma_{p_{1,j}}} \frac{1}{\sigma_{p_{2,j}}} \frac{1}{\sqrt{2\pi}} \exp\left(\frac{-(p_1 - p_{1,j})^2}{2\sigma_{p_{1,j}}^2}\right) \times$$

$$\exp\left(\frac{-(p_2 - p_{2,j})^2}{2\sigma_{p_{2,j}}^2}\right)$$

where N is the number of change-point segments, t_j is the time duration of each change-point segment, $t_{total} = \sum_{j=1}^{N} t_j$, and p_i and $\sigma_{i,j}$ represent the values of the parameters and their standard deviations, respectively, over the jth segment determined from change-point analysis. For the intensity and lifetime, the $\sigma_{i,j}$ are derived from the Fisher information expressions.[9] For the linear and color dichroism, the $\sigma_{i,j}$ are derived from propagating the error of the Poisson-distributed emission intensity uncertainties from the three channels. In constructing the probability distribution maps, the parameters over each segment are treated as Gaussian random variables. If the variables are uncorrelated then the resulting density map will either exhibit a horizontal line or a vertical line; deviations from these two limiting cases will be indicative of a correlation between the two parameters.

A typical 5 ms binned intensity−time trajectory from the nanoparticles studied is shown Figure 2A. By eye, this trajectory shows the intensity switching between bright and dark states. Figure 2B−D show the form of the data, the parameters calculated as a function of change-point segment plotted versus time. The probability maps relating the four observables, lifetime, intensity, color dichroism, and linear dichroism are plotted in Figure 3A−D. Although there are considerable variations from quantum dots to quantum dots, there are some general features that are consistent throughout those studied.
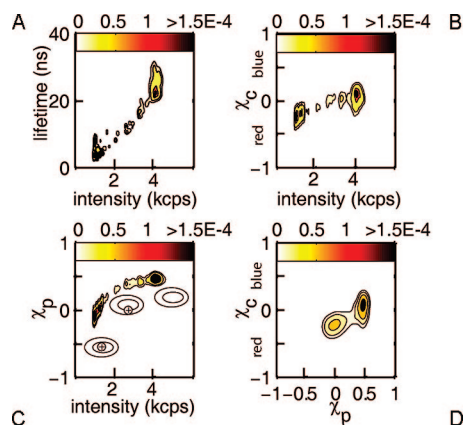

Figure 3. (A) Joint probability map for luminescence lifetime vs intensity plot for the trajectory shown in Figure 2A. kcps stands for kilocounts/s. Consistent with previous results, there is a continuous distribution of intensity states. (B) Joint probability map for color dichroism and intensity. Red-shifting of the observed luminescence occurs continuously with decreasing intensity. (C) Joint probability map for linear dichroism and intensity. The degree of linear polarization of the emitted light occurs continuously with increasing intensity. The cartoons illustrate the current working model relating a charged quantum dot to its emission characteristics, in which the quantum dot becomes nonemissive only when the charge is localized at the CdSe core. (D) Joint probability map for color dichroism and linear dichroism shows two dense populations. In all plots, the darkest color represents the saturation value such that all probabilities greater than the threshold specified are given the same maximum value. Colors less than the saturation value are distributed linearly.

From the binned intensity trajectory in Figure 2A, one sees what appear to be two states. One would therefore expect to see two dominant populations in the correlations maps. In Figure 3, all the plots show evidence of two dense populations. A closer examination reveals that there is a continuous distribution of states connecting the two dominant populations, consistent with previous results.[9] Because the intensity has been shown to be correlated to the lifetime, the plots of lifetime versus color and linear dichroism have been omitted for clarity even though they show the same general continuous distribution.

In the present study, information about the lifetime, intensity, color, and linear dichroism of the emitted luminescence were recovered as a function of time on single dots. Consistent with the idea of a continuous distribution of intensities and lifetimes (cf., Figure 3A), parts B and C of Figure 3 show a continuous distribution of spectral and polarization shifts within the intensity trajectory from a single dot. That the high-intensity state appears to show a well-defined emission polarization can be attributed to the rodlike morphology of the quantum dot sample used,[21] which has been previously shown to have an aspect ratio close to ~2.[9] Figure 3D further shows that the blue emission spectral shift is correlated with polarized emission. Note that when the particle is in its nonemissive state, only background and detector dark counts were recorded and therefore the signal, as expected, appears unpolarized. These observations are consistent with the idea of a charged dot can be emissive, but the physical location of the charge (most likely a hole state) can lead to a variety of emission characteristics.[6,27] Within this framework, one expects that the migration of a charge in the dot should mitigate the electric field to cause time-dependent fluctuations in polarization. In Figure 3, parts B and C, one sees continuous distributions of probability between intensity and the color and linear dichroism, respectively. In the figure, the probability plot shows increasing red-shifting of the spectrum with decreasing emission intensity. This is consistent with previous reports showing increasing red-

shifting of the spectrum[28,29] and concomitant red-shifting and darkening of the luminescence with an applied electric field.[29]

One of the complications in this experiment is the identification of single quantum dots using far-field optics; in particular, it has been shown using combined atomic force microscopy and optical detection that aggregates of quantum dots can display complex blinking statistics, whereas single quantum dots tend to show well-resolved two-state-like emission behavior.[30] The presence of single dots was inferred from the intensity traces which qualitatively show the presence of two dominant states (Figure 2A). The density maps in Figure 3A−D also show only two densely populated states with a continuous distribution of less populated states connecting the two (Figure 3A−D). From these data, the presence of a single dot within the diffraction volume is inferred. Future studies combining single-particle spectroscopy with simultaneous atomic force microscopy or some other imaging technique with higher spatial resolution should provide further insight on the nature of the emission and correlate them with the morphology of the particle. A careful study of the power dependence of the correlation between the different spectroscopic observables will also provide insightful information into the underlying mechanism.

In summary, the degree of emission polarization from individual quantum dots has been shown to correlate with the luminescence intensity. While the highly emissive states show highly polarized emission, the low-emissive states exhibit partially polarized light and correlate well with red-shifted spectrum and shortened luminescence lifetime—all are consistent with a model where variations of the local charge(s) around the quantum dot can lead to fluctuations in the local electric field. Understanding the fluctuations in the photophysical behavior of single quantum dots is important for such potential applications as probing and characterizing the chemical and physical properties of heterogeneous local environments, particularly how the environment may evolve over time.[31−34] Future experiments integrating three-dimensional single-particle tracking[31,35] with time-resolved studies maybe able to characterize the spectroscopic observables free of surface effects and provide a more detailed understanding of the correlation between the different spectroscopic observables presented in the paper.

References and Notes

(1) Nirmal, M.; Babbousi, B. O.; Bawendi, M. G.; Macklin, J. J.; Trautman, J. K.; Harris, T. D.; Brus, L. E. *Nature* **1996**, *383*, 802.

(2) Kuno, M.; Fromm, D. P.; Hamann, H. F.; Gallagher, A.; Nesbitt, D. J. *J. Chem. Phys.* **2000**, *112*, 3117.

(3) Kuno, M.; Fromm, D. P.; Hamann, H. F.; Gallagher, A.; Nesbitt, D. J. *J. Chem. Phys.* **2001**, *115*, 1028.

(4) Empedocles, S. A.; Bawendi, M. G. *Science* **1997**, *278*, 2114.

(5) Empedocles, S. A.; Bawendi, M. G. *J. Phys. Chem. B* **1999**, *103*, 1826.

(6) Neuhauser, R. G.; Shimizu, K. T.; Woo, W. K.; Empedocles, S. A.; Bawendi, M. G. *Phys. Rev. Lett.* **2000**, *85*, 3301.

(7) Schlegel, G.; Bohnenberger, J.; Potapova, I.; Mews, A. *Phys. Rev. Lett.* **2002**, *88*, 137401.

(8) Fisher, B. R.; Eisler, H.-J.; Stott, N. E.; Bawendi, M. G. *J. Phys. Chem. B* **2004**, *108*, 143.

(9) Zhang, K.; Chang, H.; Fu, A.; Alivisatos, A. P.; Yang, H. *Nano Lett.* **2006**, *6*, 843.

(10) Cichos, F.; von Borczyskowski, C.; Orrit, M. *Curr. Opin. Colloid Interface Sci.* **2007**, *12*, 272.

(11) Efros, A. L.; Rosen, M. *Phys. Rev. Lett.* **1997**, *78*, 1110.

(12) Shimizu, K. T.; Neuhauser, R. G.; Leatherdale, C. A.; Empedocles, S. A.; Woo, W. K.; Bawendi, M. G. *Phys. Rev. B* **2001**, *63*, 205316.

(13) Tang, J.; Marcus, R. A. *J. Chem. Phys.* **2005**, *123*, 054704.

(14) Frantsuzov, P. A.; Marcus, R. A. *Phys. Rev. B* **2005**, *72*, 155321.

(15) Margolin, G.; Protasenko, V.; Kuno, M.; Barkai, E. *J. Phys. Chem. B* **2006**, *110*, 19053.

(16) Pelton, M.; Smith, G.; Scherer, N. F.; Marcus, R. A. *Proc. Natl. Acad. Sci. U.S.A.* **2007**, *104*, 14249.

(17) Knappenberger, K. L., Jr.; Wong, D. B.; Romanyuk, Y. E.; Leone, S. R. *Nano Lett.* **2007**, *7*, 3869.

(18) Issac, A.; von Borczyskowski, C.; Cichos, F. *Phys. Rev. B* **2005**, *71*, 161302.

(19) Krauss, T. D.; Brus, L. *Phys. Rev. Lett.* **1999**, *83*, 4840.

(20) Chung, I.; Shimizu, K. T.; Bawendi, M. G. *Proc. Natl. Acad. Sci. U.S.A.* **2003**, *100*, 405.

(21) Hu, J.; Li, L.-S.; Yang, W.; Mana, L.; Wang, L.-W.; Alivisatos, A. P. *Science* **2001**, *292*, 2060.

(22) Axelrod, D. *Biophys. J.* **1979**, *26*, 557.

(23) Wei, C. Y. J.; Kim, Y. H.; Darst, R. K.; Rossky, P. J.; Vanden Bout, D. A. *Phys. Rev. Lett.* **2005**, *95*, 173001.

(24) Yang, H. *J. Phys. Chem. A* **2007**, *111*, 4987.

(25) Watkins, L. P.; Yang, H. *J. Phys. Chem. B* **2005**, *109*, 21930.

(26) Wustholz, K. L.; Bott, E. D.; Kahr, B.; Reid, P. J. *J. Phys. Chem. C* **2008**, *112*, 7877.

(27) Verbek, R.; van Oijen, A. M.; Orrit, M. *Phys. Rev. B* **2002**, *66*, 233202.

(28) Müller, J.; Lupton, J. M.; Rogach, A. L.; Feldmann, J.; Talapin, D. V.; Weller, H. *Phys. Rev. B* **2005**, *72*, 205339.

(29) Rothenberg, E.; Kazes, M.; Shaviv, E.; Banin, U. *Nano Lett.* **2005**, *5*, 1581.

(30) Yu, M.; Van Orden, A. *Phys. Rev. Lett.* **2006**, *97*, 237402.

(31) Cang, H.; Xu, C. S.; Montiel, D.; Yang, H. *Opt. Lett.* **2007**, *32*, 2729.

(32) Li, S.; Zhang, K.; Yang, J.-M.; Lin, L.; Yang, H. *Nano Lett.* **2007**, *7*, 3102.

(33) Nan, X.; Sims, P. A.; Chen, P.; Xie, X. S. *J. Phys. Chem. B* **2005**, *109*, 24220.

(34) Tsay, J. M.; Doose, S.; Weiss, S. *J. Am. Chem. Soc.* **2006**, *128*, 1639.

(35) McHale, K.; Berglund, A. J.; Mabuchi, H. *Nano Lett.* **2007**, *7*, 3535.